Histol Histopathol (2017) 32: 1065-1076

http://www.hh.um.es

Histology and Histopathology

From Cell Biology to Tissue Engineering

ERK1/2, JNK and STAT3 activation and correlation with tumor differentiation in oral SCC

I. Gkouveris[1], N. Nikitakis[1], D. Avgoustidis[2], M. Karanikou[3], G. Rassidakis[3] and A. Sklavounou[1]

[1]Department of Oral Pathology and Medicine, Dental School, National and Kapodistrian University of Athens, [2]Department of Oral and Maxillofacial Surgery, "Evaggelismos" Hospital, National and Kapodistrian University of Athens and [3]First Department of Pathology, Medical School, National and Kapodistrian University of Athens, Athens, Greece

Summary. Signal transducer and activator of transcription 3 (STAT3) and mitogen activated protein kinases (MAPKs), including ERK and JNK, have been implicated in oral squamous cell carcinoma (OSCC) development and progression. Our purpose was to evaluate the levels of activated STAT3, ERK1/2 and JNK by immunohistochemistry in OSCC and to investigate possible correlations of these molecules with each other as well as with the degree of tumor differentiation.

Immunohistochemical assessment of the phosphorylated levels of STAT3(tyrosine/ serine), ERK1/2 and JNK was performed in 60 OSCC, including well, moderately and poorly differentiated tumors. Semi-quantitative scoring system was used, by calculating intensity of immunostaining, percentage of positive cells and combined scores. Statistics included Fisher's test, Student's T-Test and Kruskal-Wallis analysis, Spearman's correlation coefficient and multivariate logistic regression analyses.

Immunohistochemical levels of both pSTAT3(tyr) and pERK1/2 showed statistically significant differences between well and poorly differentiated tumors with the latter receiving higher mean percentage, intensity and total scores. On the other hand, pJNK showed statistically significantly higher intensity levels in moderately compared to poorly differentiated tumors. pSTAT3(ser) immunoexpression did not appear to correlate with tumor differentiation. Between different molecules, more pronounced, pERK1/2 levels exhibited statistically significant positive correlation with pSTAT3(ser), pSTAT3(tyr) and pJNK expression.

ERK1/2 and STAT3 activation (as assessed by tyrosine but not serine phosphorylation) could contribute to a less differentiated phenotype in OSCC, while JNK activation may have an opposite, although possibly less pronounced, effect. Positive correlations between MAPK and STAT3 levels may indicate a direct crosstalk and/or regulation by common upstream pathways.

Key words: MAPK, STAT3, Correlation, Tumor grade

Introduction

The signal transducer and activator of transcription (STAT) proteins are transcription factors that have been involved in oncogenesis (Abroun et al., 2015; Gkouveris et al., 2015). STATs have been found to participate in various signaling pathways, including cytokine receptor-associated kinases, growth factor receptor tyrosine kinases and non-receptor tyrosine kinases (Macha et al., 2011). STATs are present in the cytoplasm and become activated in response to stimulation by cytokines and growth factors (Gkouveris et al., 2015; Mali, 2015). STAT activation involves phosphorylation, leading to receptor dissociation, dimerization and translocation to the nucleus, where they regulate the transcription of target genes, involved in oncogenesis (Macha et al., 2011; Xiong et al., 2014).

STAT3, a major member of the STAT family, is

Offprint requests to: Dr. I. Gkouveris, Department of Oral Pathology and Medicine, Dental School National and Kapodistrian University of Ahtens, Greece. e-mail: igkouver@gmail.com

DOI: 10.14670/HH-11-868

activated in several cancers (Sen et al., 2012). In head and neck squamous cell carcinoma (HNSCC), constitutive STAT3 activation is associated with deregulation of cell cycle, enhanced proliferation and prevention of apoptosis, as well as with adverse clinical parameters (Shah et al., 2009; Macha et al., 2011; Trivedi et al., 2011). Aberrant TGF-α/EGFR signaling has been pinpointed as a major contributor to STAT3 constitutive activation in HNSCC (Kijima et al., 2002; Nikitakis et al., 2004; Leeman et al., 2006; Molinolo et al., 2009). Other lines of evidence suggest the existence of EGFR-independent mechanisms driving STAT3 oncogenic activity in HNSCC, including cytokine (IL-6, IL-10 or IL-22) stimulation or signaling through 7 nicotinic and erythropoietin receptor pathways (Lee et al., 2006; Jewett et al., 2006; Lai et al., 2010; Naher et al., 2012). STAT3 targeting has been proposed as a promising novel antineoplastic strategy for HNSCC (Nikitakis et al., 2004).

The family of mitogen-activated protein kinases (MAPK) are evolutionarily conserved kinase modules that play an essential signaling role in several cellular processes, such as differentiation, growth, proliferation, inflammation and apoptosis (Maggioni et al., 2011; Kim et al., 2012). MAPKs are classified into three major groups, including extracellular signal-regulated kinases (ERKs), p38 MAPKs, and c-Jun NH2-terminal kinases (JNKs) (Aguzzi et al., 2009). Aberrant MAPK signaling has been implicated in several types of cancer, including HNSCC (Dhillon et al., 2007; Aguzzi et al., 2009; Maggioni et al., 2011).

ERKs, activated by various oncoproteins, such as Ras and Raf (Chen et al., 2001; Maggioni et al., 2011), have been shown to play a role in various types of cancer, such as liver, prostate and malignant melanoma cancer, driving cell growth *in vitro* and *in vivo* (Smalley et al., 2003; Bessard et al., 2008; Obajimi and Melera et al., 2010). Downstream targets of ERKs include the p90 ribosomal S6 kinase, the ternary complex factor (TCF), transcription factors and the family of Mitogen and Stress-activated Protein Kinases (MSKs) (Anjum and Blenis, 2008; Maggioni et al., 2011; Mendoza et al., 2011). The significance of the MEK/ERK pathway in HNSCC has been supported by several studies highlighting ERK participation in cell cycle regulation, cell proliferation and apoptosis alterations (Wang et al., 2006; Lin et al., 2012; Ji et al., 2014).

JNK kinases are involved in cellular stress response and apoptosis (Chang et al., 2001; Chen et al., 2009), but their role in malignant transformation is still under investigation (Gkouveris et al., 2014). While some authors consider that activation of the JNK signaling pathway can lead to apoptotic or non-apoptotic cell death (Sau et al., 2012; Chen et al., 2013; Sui et al., 2014), others propose that JNKs promote cell transformation and proliferation in cancer (Chen, 2012). Similarly, JNK signaling has been studied in HNSCC with controversial findings (Gross et al., 2007; Boivin et al., 2011; Yunoki et al., 2013).

Overall, there is compelling evidence to suggest that specific MAPKs and STAT3 play an important role in HNSCC. The aim of the present investigation was to evaluate the frequency and significance of STAT3 activation (through tyrosine and serine phosphorylation), in correlation with JNK and ERK1/2 expression and activation in oral squamous cell carcinomas (OSCCs) of various degrees of differentiation.

Materials and methods

Materials

The study material comprised sixty OSCC cases obtained from established tissue repository of the Department of Oral Pathology and under the auspices of tissue bank protocol approved by the National and Kapodistrian University of Athens, Greece, Institutional Review Board. The tumors were classified according to Anneroth's grading system into well (WD), moderate (MD) and poorly differentiated (PD) (3 groups of 20).

Immunohistochemical staining

Paraffin-embedded tissue sections of tumor samples were deparaffinized, immersed in ethanol 100% and 95%, and heated for antigen retrieval in 0.01 M citrate buffer (C2488, Sigma-Aldrich) for 25 minutes in a pressure cooker inside a microwave oven. After dehydration in hydrogen peroxide, the sections were incubated with primary antibodies at room temperature for 1 hour. The applied antibodies were polyclonal phospho-STAT3 (Tyr705) (1:100) (Cell Signaling, Beverly, MA, USA#9131), polyclonal phospho-STAT3 (Ser727) (1:100) (Cell Signaling, Beverly, MA, USA #9134), monoclonal phospho-cJunNH2-terminal Kinase (sc6254) (1:200) (Santa Cruz Bio.inc), monoclonal phospho-ERK1/2(1:300) (Cell Signaling, Beverly, MA, USA # 4370). To validate the staining in HNSCC samples, positive controls of tissue sections known to express the four studied proteins were used (Breast cancer for pSTAT3 tyr/ser, Endometrial cancer for pJNK and Melanoma for pERK1/2).

Standard streptavidin–biotin–peroxidase complex method was employed to bind to the primary antibody along with multilink concentrated biotinylated anti-IgG as secondary antibody (1:2000, rabbit anti-Human IgG, ThermoFisher Scientific). Reaction products were visualized by counterstaining with the 3,3V-diaminobenzidine reagent set (Kirkegaard and Perry Laboratories, Gaithersburg, MD). Sections were counterstained with hematoxylin. As a negative control, sections were treated with PBS, with the omission of the primary antibody. Additionally, tumors were stained with Harris' hematoxylin (Harleco, Kansas City, MO) and eosin (Sigma Chemical Co.) for microscopic evaluation. Immunostains were reviewed by 3 independent evaluators (NN, GR, IG).

Positive criterion for immunohistochemical staining

The immunopositive staining was evaluated in 5 randomly selected areas of the tissue section and specific staining in cancer cells was defined as positive staining. Sections were scored as positive if cancer cells showed immunopositivity in the nucleus when observed by all 3 evaluators, independently, who were blinded to grading of the tissue samples, while scoring the immunoreactivity. The tissue sections were scored based on the percentage of immunostained cells as: 0% to 10% =0; 10% to 30% =1; 30% to 50% =2; 50% to 70%= 3; and 70% to 100% =4. Sections were also scored on the basis of staining intensity as negative =0; mild=1; moderate= 2; intense= 3. To validate staining intensity in HNSCC samples, positive controls of previously studied tissues known to express the four proteins were used and their intensity was classified as moderate. Lower intensity (light brown) compared to the brown staining of the positive control was classified as weak, while higher intensity (dark brown) compared to the positive control was classified as strong. Finally, a total score was obtained by adding the score of percentage positivity and intensity.

Twenty non-malignant tissues (with histologically confirmed normal oral epithelium) were also evaluated for all 4 proteins expression (control). The source of normal tissues was from adjacent normal epithelium of routinely surgically excised traumatic fibromas of patients with no smoking or alcohol consumption habits.

Statistical analysis

The baseline characteristics of patients were summarized as mean and standard deviation (SD) for continuous or ordinal data and as absolute (n) and relative (%) frequency for categorical variables.

The two tailed Fisher's exact test was performed in order to evaluate possible differences in the frequency distribution of clinical and pathologic features of patients between men and women, as well as in the frequency distribution of cases with positive and negative IHC staining between the three groups of tumor differentiation.

Comparisons concerning the age of patients were based on Student's t-test, while ordinal data were compared with the use of the Kruskal-Wallis one way analysis of variance by ranks. Post-hoc pairwise comparisons after a significant Kruskal-Wallis test were carried out with the application of Dunn's test.

Spearman's rank correlation coefficient rho (r) was calculated for the evaluation of possible correlations between the ranks of the various IHC scores for every single molecule under study with the progression of tumor differentiation, as well as the correlations between IHC expression patterns between molecules for every grade of tumor differentiation.

Univariate logistic regression models were calculated in an effort to assess whether the various IHC expression levels of the proteins under study could serve as predictors of tumor differentiation. These models were separately calculated for every protein and for every type of IHC expression pattern.

Multivariate logistic regression analyses, using the forward Wald method, attempted to evaluate the contribution of selected parameters of IHC staining in predicting tumor differentiation. Based on previous univariate analyses findings, six models were calculated, three for well differentiated tumors and another three for the poorly differentiated ones. Every model evaluated concurrently either the intensity scores, the percentage scores or the combined scores of those molecules which were proven to serve as significant predictors for tumor grade from the univariate analyses. Multivariate logistic regression analyses were also applied in order to calculate the Odds Ratio (OR) and 95% Confidence Intervals (95% CI) of the variables retained in the final regression models.

The Hosmer and Lemeshow Goodness of Fit test (HLGFT) was applied in order to quantify the chi-square value and statistical significance of all regression models constructed.

Statistical analyses were performed using the SPSS® software application (version 21.0; IBM® SPSS Statistics, Chicago, IL, USA) with $P<0.05$ as the threshold of significance.

Results

Study sample patients' demographics

The frequency distribution of selected characteristics of the patients whose biopsy specimens comprised the study sample are presented in Table 1, according to gender. The sample consisted of 60 cases, namely 33 men (55.0%) and 27 women (45.0%). The mean age was 61.2 years (±7.8 years; range, 42-73 years) for men and 63.4 years (±9.3 years; range, 40-83 years) for women.

Table 1. Frequency distributions of selected demographic variables according to gender.

Characteristics	Men	Women	P	Total
n	33 (55.0%)	27 (45.0%)		60 (100%)
Age:				
Mean (±S.D.)	61.2 (±7.8)	63.4 (±9.3)	0.323*	62.2 (±8.5)
Range	42 - 73	40 - 83		40 - 83
Tumor site:				
Tongue	21 (35.0%)	19 (31.7%)	0.677**	40 (66.7%)
Floor of mouth	7 (11.7%)	6 (10.0%)		13 (21.7%)
Alveolar crest	5 (8.3%)	2 (3.3%)		7 (11.6%)
Positive history of:				
Smoking	25 (41.7%)	23 (38.3%)	0.519**	48 (80.0%)
Alcohol intake	15 (25.0%)	8 (13.3%)	0.189**	23 (38.3%)

S.D.: Standard Deviation. * Student's t-test. **Two tailed Fisher's exact test.

Mean ages between these two groups were comparable (P=0.323). A non-statistically significant distribution according to tumor site and the history of smoking and alcohol intake was also observed between men and women, as can be deduced from Table 1.

Immunohistochemical (IHC) expression patterns and their correlation with tumor grade

pSTAT3(tyr)

IHC staining was positive in 70.0% (14/20), 85.0% (17/20) and 88.8% (16/20) of WD, MD and PD cases, respectively. The PD cases showed the highest mean scores in all three studied variables: staining intensity, percentage of cells and combined score, as opposed to WD cases which showed the corresponding lower scores. Data are given in Table 2.

The application of Kruskal-Wallis test revealed that the distribution of pSTAT3(tyr) intensity, percentage and combined scores differed across the categories of tumor differentiation at a statistically significant level, as can also be seen in Table 2 (Intensity Score P=0.009; Percentage Score P=0.027; Combined Score P=0.003). Post–hoc pairwise comparisons with the help of Dunn's test attributed these differences only between WD and PD tumors for all types of IHC scores (WD vs PD Intensity Score P=0.007; WD vs PD Percentage Score P=0.022; WD vs PD Combined Score P=0.002).

Furthermore, the application of Spearman's Rank correlation coefficient test revealed a positive type of correlation between all IHC scores (intensity, percentage and combined) and the progression of tumor grade, as shown in Table 3 (Intensity Score r=0.417, P=0.002; Percentage Score r=0.366, P=0.006; Combined Score r=0.463, P<0.001).

pSTAT3(ser)

IHC staining was positive in 85.0% (17/20), 95% (19/20) and 90.0% (18/20) of WD, MD and PD cases, respectively. The PD cases showed the highest mean scores in all three studied variables, as depicted in Table 2. However, these differences were not statistically significant with the application of Kruskal-Wallis test. Moreover, no statistically significant association was detected between the various pSTAT3(ser) IHC scores and the tumor differentiation levels, as can be seen in Table 3.

pERK1/2

IHC staining was positive in 70.0% (14/20), 100% (20/20) and 85.0% (17/20) of WD, MD and PD tumors, respectively. The frequency distribution of samples with positive IHC staining was significantly different across the categories of tumor grade (P=0.025). The PD cases showed the highest mean scores in all three studied variables, as opposed to WD, which showed the corresponding lower scores. These results are given in Table 2.

Statistical analysis revealed that the distribution of pERK1/2 intensity, percentage and combined scores differed across the categories of tumor differentiation at a statistically significant level (Intensity Score P=0.030; Percentage Score P=0.001; Combined Score P=0.001). Post–hoc pairwise comparisons after Kruskal-Wallis test revealed that all IHC scores of pERK1/2 showed statistically significant differences between WD and PD

Table 2. Frequency distribution of cases with positive immunohistochemistry staining for pSTAT3(tyr), pSTAT3(ser), pERK1/2 and p-JNK according to tumor differentiation, as well as their relative IHC mean score values (±SD).

		Tumor Differentiation Status				Total sample
		Well (n=20)	Moderate (n=20)	Poor (n=20)	P	(n=60)
pSTAT3 (tyr)	n (%) of cases with positive IHC staining	14 (70.0%)	17 (85.0%)	16 (80.0%)	0.588*	47 (78.3%)
	Intensity Score (±SD)	1.05 (±0.85)	1.61 (±0.85)	2.06 (±1.06)	0.009**	1.56 (±0.99)
	Percentage Score (±SD)	1.16 (±1.02)	1.61 (±0.85)	2.06 (±1.06)	0.027**	1.60 (±1.03)
	Combined Score (±SD)	2.21 (±1.58)	3.22 (±1.40)	4.17 (±1.95)	0.003**	3.18 (±1.81)
pSTAT3 (ser)	n (%) of cases with positive IHC staining	17 (85.0%)	19 (95.0%)	18 (90.0%)	0.689*	54 (90.0%)
	Intensity Score (±SD)	2.22 (±1.00)	2.30 (±0.92)	2.50 (±0.71)	0.763**	2.34 (±0.88)
	Percentage Score (±SD)	1.72 (±0.90)	2.05 (±0.95)	2.17 (±0.79)	0.301**	1.98 (±0.88)
	Combined Score (±SD)	3.94 (±1.60)	4.35 (±1.60)	4.67 (±1.19)	0.319**	4.32 (±1.48)
pERK1/2	n (%) of cases with positive IHC staining	14 (70.0%)	20 (100%)	17 (85.0%)	0.025*	51 (85.0%)
	Intensity Score (±SD)	1.78 (±1.26)	2.35 (±0.88)	2.72 (±0.75)	0.030**	2.29 (±1.04)
	Percentage Score (±SD)	1.06 (±0.80)	1.90 (±0.85)	2.22 (±0.88)	0.001**	1.73 (±0.96)
	Combined Score (±SD)	2.83 (±1.86)	4.25 (±1.55)	5.00 (±1.53)	0.001**	4.04 (±1.85)
p-JNK	n (%) of cases with positive IHC staining	16 (80.0%)	18 (90.0%)	15 (75.0%)	0.589*	49 (81.7%)
	Intensity Score (±SD)	2.06 (±0.99)	2.25 (±0.97)	1.42 (±1.07)	0.037**	1.91 (±1.06)
	Percentage Score (±SD)	1.94 (±0.99)	1.85 (±1.04)	1.58 (±1.07)	0.547**	1.79 (±1.03)
	Combined Score (±SD)	4.00 (±1.85)	4.05 (±1.91)	3.00 (±2.08)	0.180**	3.68 (±1.97)

S.D.: Standard Deviation. *Two tailed Fisher's exact test. **Kruskal-Wallis test.

tumors (WD vs PD Intensity Score P=0.025, WD vs PD Percentage Score P=0.001, WD vs PD Combined Score P<0.001). In addition, pERK1/2 percentage score was also significantly higher in MD tumors compared to WD tumors (P=0.025).

All types of pERK1/2 IHC scores were positively associated with tumor progression as can be deduced from Table 3 (Intensity Score r=0.357, P=0.007; Percentage Score r=0.496, P<0.001; Combined Score r=0.508, P<0.001).

p-JNK

IHC staining was positive in 80.0% (16/20), 90% (18/20), and 75.0% (15/20) in WD, MD and PD tumors, respectively. The mean average scores of all three IHC variables were lower in PD tumors, as shown in Table 2. While p-JNK percentage and combined scores did not show any statistically significant differences between the various tumor differentiation categories, the p-JNK Intensity Score differed at a statistically significant level (P=0.037). Post–hoc pairwise comparisons attributed this difference to the PD and MD tumor groups (P=0.041). No correlation was found between p-JNK IHC scores and the progression of tumor differentiation, as can be seen in Table 3.

Univariate logistic regression analyses for the evaluation of the IHC score types as predictors of tumor differentiation

The possibility that the IHC expression levels of specific proteins can serve as predictors of tumor differentiation was also evaluated by univariate analyses based on the different types of IHC scores. Therefore, nine different univariate logistic regression models were calculated for all three categories of tumor differentiation, based on the intensity, percentage and combined IHC scores of every single molecule. These data are shown in Table 4.

Based on this type of analysis, pSTAT3(tyr) and pERK1/2 IHC scores serve as significant predictors only for well and poorly differentiated tumors, taking into account that these scores were negatively associated with well differentiated tumors and positively associated with the poorly differentiated ones. Therefore, as these scores increase, the odds of 'predicting' a PD tumor also increase. Conversely, p-JNK intensity score levels serve as predictor only for poorly differentiated tumors in an inverse manner: tumors with positive p-JNK staining had double the odds not to be poorly differentiated (OR: 0.50, 95% CI: 0.29 - 0.88).

Multivariate logistic regression analysis for predicting tumor differentiation

In all series of models for well differentiated tumors, intensity, percentage and combined scores of

Table 3. Correlation of the progression of tumor differentiation and the various types of IHC scores for pSTAT3(tyr), pSTAT3(ser), p-ERK1/2 and p-JNK.

Molecule under study	Association of tumor differentiation progression with:					
	Intensity Score		Percentage Score		Combined Score	
	r*	P	r*	P	r*	P
pSTAT3(tyr)	0.417	0.002	0.366	0.006	0.463	<0.001
pSTAT3(ser)	0.094	0.490	0.198	0.144	0.199	0.141
pERK1/2	0.357	0.007	0.496	<0.001	0.508	<0.001
p-JNK	-0.246	0.065	-0.0142	0.291	-0.206	0.124

r*: Spearman's Rank correlation coefficient rho

Table 4. Univariate logistic regression analysis for predicting the category of tumor differentiation (well, moderate and poor) based on the various scores from IHC expression patterns for pSTAT3(tyr), pSTAT3(ser), pERK1/2 and p-JNK.

IHC parameters		Category of tumor differentiation					
		Well		Moderate		Poor	
		P	OR (95% CI)	P	OR (95% CI)	P	OR (95% CI)
Intensity Scores	pSTAT3(tyr)	0.009	0.40 (0.20-0.80)	0.803	N.C.	0.014	2.27 (1.18-4.37)
	pSTAT3(ser)	0.489	N.C.	0.802	N.C.	0.342	N.C.
	pERK1/2	0.016	0.50 (0.29-0.88)	0.728	N.C.	0.043	2.22 (1.02-4.82)
	p-JNK	0.483	N.C.	0.074	N.C.	0.017	0.50 (0.29-0.88)
Percentage Scores	pSTAT3(tyr)	0.025	0.49 (0.27-0.91)	0.955	N.C.	0.026	2.01 (1.09-3.70)
	pSTAT3(ser)	0.127	N.C.	0.666	N.C.	0.278	N.C.
	pERK1/2	0.001	0.25 (0.11-0.59)	0.326	N.C.	0.012	2.42 (1.22-4.80)
	p-JNK	0.408	N.C.	0.742	N.C.	0.271	N.C.
Combined Scores	pSTAT3(tyr)	0.007	0.60 (0.41-0.87)	0.908	N.C.	0.008	1.72 (1.15-2,56)
	pSTAT3(ser)	0.185	N.C.	0.913	N.C.	0.225	N.C.
	pERK1/2	0.002	0.57 (0.39-0.82)	0.514	N.C.	0.013	1.78 (1.13-2.79)
	p-JNK	0.408	N.C.	0.300	N.C.	0.062	N.C.

OR: Odds Ratio; 95% CI: 95% Confidence Interval; N.C.: Non calculable data.

pSTAT3(tyr) and pERK1/2 were concurrently evaluated. For the poorly differentiated tumor models the same parameters were also evaluated synchronously, with the addition of the p-JNK intensity score in the respective model. All models were further tested with the application of Hoshmer and Lemeshow goodness of fit test (HLGFT).

The various IHC parameters of pERK1/2 served as the sole significant predictor in the well differentiated tumor models, outweighing the pSTAT3(tyr) IHC parameters. In detail, the pERK1/2 scores were inversely associated with well differentiated tumors in the intensity of staining model (P=0.006, OR=0.40, 95% CI: 0.20-0.77, HLGFT P=0.403), percentage of cells score model (P=0.001, OR=0.19, 95% CI: 0.07-0.50, HLGFT P=0.649) and combined score model (P=0.001, OR=0.45, 95% CI: 0.28-0.73, HLGFT P=0.148), respectively.

Analogous findings were also noticed for all three poorly differentiated tumor models with the exception of the intensity of staining model. In this model both pERK1/2 intensity of staining score (P=0.010, OR: 7.83, 95% CI: 1.63-37.49), as well as p-JNK intensity of staining score (P=0.003, OR: 0.270, 95% CI: 0.11-0.64) serve as significant predictors for the poorly differentiated tumors when they are evaluated concurrently (HLGFT P=0.890). Moreover, pERK1/2 intensity of staining score is positively associated with poorly differentiated tumors, while the respective p-JNK score is inversely associated. Concerning the percentage of cells score model, only the pERK1/2 percentage score served as predictor for poorly differentiated tumors (P=0.006, OR: 2.93, 95% CI: 1.35-6.34, HLGFT P=0.509). In the same pattern the pERK1/2 combined score served as the sole predictor for poorly differentiated tumors in the respective combined scores model (P=0.006, OR: 2.42, 95% CI: 1.29-4.54, HLGFT P=0.836).

Correlation between IHC expression of various molecules with each other according to tumor differentiation

Possible correlation between IHC expression of all studied molecules was also evaluated in a pair-wise manner by Spearman's Correlation Coefficient test for all tumors as well as for each tumor grade separately (Table 5).

Considering all tumor grades together, all pERK1/2 IHC scores (percentage, intensity and combined) were positively correlated at a statistically significant level with the corresponding scores for pSTAT3(ser), pSTAT3(tyr) and pJNK. In addition, a statistically significant positive correlation between pSTAT3(ser) and pJNK intensity scores was also noted.

In particular, well differentiated tumors demonstrated statistically significant positive correlations for IHC combined scores between pSTAT3(ser) and pSTAT3(tyr), pSTAT3(ser) and pERK1/2, pSTAT3(tyr) and pERK1/2, pSTAT3(ser) and pJNK, as well as between pERK1/2 and pJNK. In contrast, no significant correlations were seen in moderately and poorly differentiated tumors regarding combined scores; the only observed correlations were between pERK1/2 and p-JNK intensity scores in moderately differentiated tumors and between pSTAT3(tyr) and pERK1/2 percentage scores in poorly differentiated tumors (Figs. 1, 2).

Table 5. Correlation between the immunohistochemical expression parameters (intensity, percentage and total scores) of the studied molecules in OSCC (according to tumor differentiation).

IHC parameters	Well		Moderate		Poor		Total	
	r*	P	r*	P	r*	P	r*	P
Intensity of staining scores								
pSTAT3(ser) & pSTAT3(tyr)	0.697	0.002	-		-		-	
pSTAT3(ser) & pERK1/2	0.517	0.040	-		-		0.268	0.050
pSTAT3(tyr) & pERK1/2	-		-		-		0.385	0.005
pSTAT3(ser) & pJNK	0.529	0.024	-		-		0.268	0.045
pERK1/2 & pJNK	0.779	<0.001	0.492	0.027	-		0.389	0.004
Percentage of cells scores								
pSTAT3(tyr) & pERK1/2	0.502	0.040	-		0.628	0.007	0.545	<0.001
pSTAT3(ser) & pERK1/2	-		-		-		0.289	0.034
pERK1/2 & pJNK	-		-		-		0.297	0.029
Combined IHC scores								
pSTAT3(ser) & pSTAT3(tyr)	0.491	0.045	-		-		-	
pSTAT3(ser) & pERK1/2	0.684	0.004	-		-		0.311	0.022
pSTAT3(tyr) & pERK1/2	0.660	0.004	-		-		0.484	<0.001
pSTAT3(ser) & pJNK	0.549	0.018	-		-		-	
pERK1/2 & pJNK	0.710	0.002	-		-		0.329	0.015

r*: Spearman's Rank correlation coefficient rho; Only the pairs of proteins with a statistical significant correlation are given.

Discussion

STAT3 signaling has been involved in HNSCC oncogenesis (Kijima et al., 2002; Nikitakis et al., 2004; Leeman et al., 2006; Molinolo et al., 2009). Specifically, aberrant STAT3 tyrosine phosphorylation, driven from

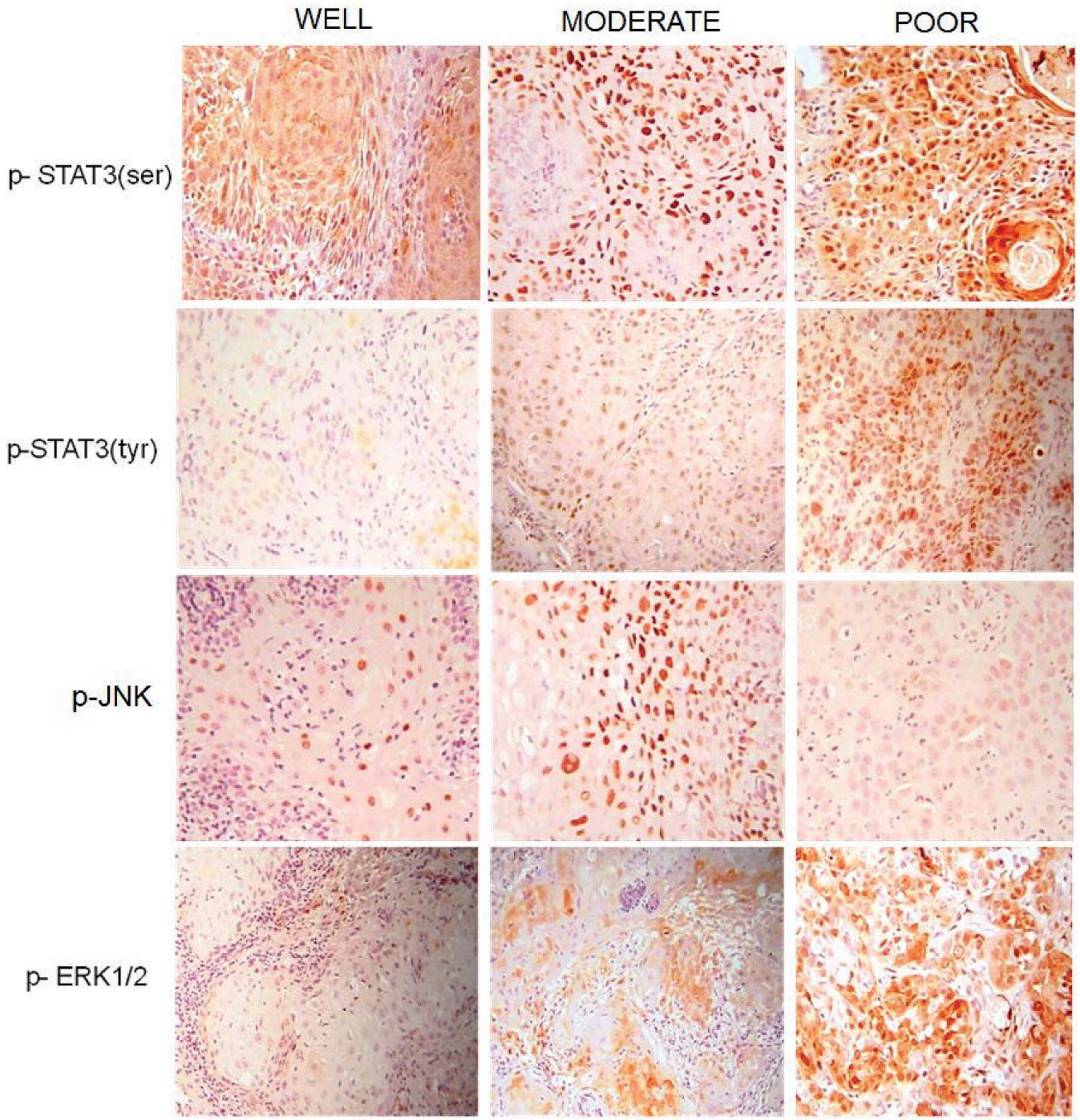

Fig. 1. Indicative staining for all 4 proteins applied including well, moderate and poor differentiated cases. Immunohistocemical staining of the studied molecules pSTAT3(tyr), pSTAT3(ser), pERK1/2 and pJNK in OSCC. Representative photomicrographs for each molecule in well, moderately and poorly differentiated tumors are depicted. Overall, poorly differentiated cases showed higher immunohistochemical scores for pSTAT3(tyr) and pERK1/2. In contrast, pJNK showed lower intensity levels in poorly differentiated tumors, while pSTAT3(ser) immunoexpression did not show noticeable differences among cases of variable differentiation. x 200.

dysregulated upstream (such as TGF-α/EGFR and cytokine) signaling, contributes to cell proliferation, differentiation and apoptosis abnormalities in HNSCC (Kijima et al., 2002; Leeman et al., 2006). STAT3 can also be phosphorylated in the serine 727 residue, but the role of this phosphorylation in cancer remains controversial (Reich and Liu, 2006). While some authors suggested a negative relationship between STAT3 serine and tyrosine phosphorylation (Chung et al., 1997; Lim and Cao, 1999; Venkatasubbarao et al., 2005; Wakahara et al., 2012), indicating that serine phosphorylation may counteract the oncogenic activities mediated by tyrosine phsophorylation, other lines of evidence suggest that STAT3 serine phosphorylation may contribute to higher STAT3 nuclear translocation and transcriptional activity (Siavash et al., 2004; Leeman et al., 2006), thus acting in favor of cancer promotion (Zhang et al., 2013). In HNSCC, ERK1/2-induced upregulation of STAT3 Ser727 was found to accompany the oncogenic potential of ERK1/2 (Gkouveris et al., 2014).

In the present study, high p-STAT3 (tyr) immunoexpression levels appeared to correlate with poorly differentiated tumors, serving as potential indicators of low differentiation, and supporting the

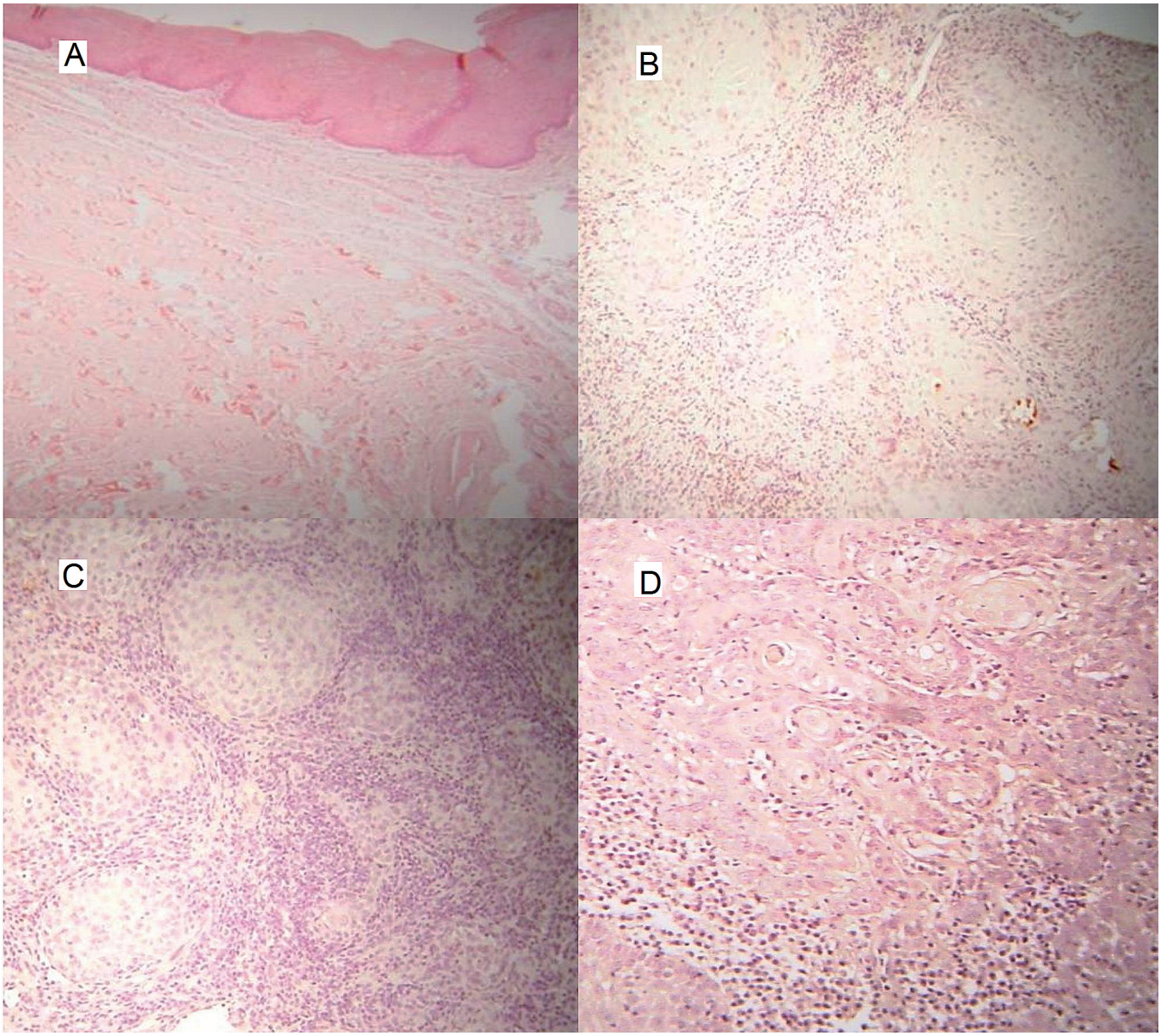

Fig. 2. Indicative staining cases used as control. No immunohistochemical expression of pSTAT3(tyr) for non-malignant tissue **(A)**. Negative immunohistochemical staining of pSTAT3(tyr) **(B)**, pERK1/2 **(C)** and pJNK (**D)** in OSCC cases. A, x 50; B-D, x 200

oncogenic role of STAT3 tyrosine phosophorylation in HNSCC. Similarly, previous immunohistochemical studies have linked high levels of p-STAT3 (tyr) expression with a low degree of differentiation (Masuda et al., 2002; Shah et al., 2006), as well as with the presence of lymph node metastases (Shah et al., 2006; Sen et al., 2012) and a poorer prognosis in HNSCC (Masuda et al., 2002; Shah et al., 2006; Sen et al., 2012). Masuda et al. (2002) also found that increased expression of p-STAT3 (tyr) was accompanied by corresponding increased levels of cyclin D1 expression (Sen et al., 2012). In addition, high levels of p-STAT3(tyr) expression in HNSCC have been associated with greater resistance to treatment with cetuximab and cisplatin (Reich and Liu, 2006; Gu et al., 2010).

On the other hand, immunohistochemical staining for p-STAT3 (ser) was positive in the vast majority of cases with considerable variation in the levels of expression. However, no significant correlation of p-STAT3 (ser) with the degree of tumor differentiation was found. To the best of our knowledge, no previous studies have investigated the immunohistochemical expression of p-STAT3 (ser) in HNSCC but the presence of p-STAT3 (ser) in almost all cases suggests a potential functional role in HNSCC, which needs to be further investigated. Regarding other tumor types, Lin et al. (2014) reported that glioblastoma patients with higher expression levels of both p-STAT3 (tyr) and p-STAT3 (ser) had a poorer prognosis; positivity of p-STAT3 (ser) was proposed as an independent unfavorable prognostic of glioblastoma cells (Lin et al., 2014). Furthermore, increased nuclear p-STAT3 (ser) expression levels correlated significantly with negative estrogen receptor status, increased stage of cancer and increased tumor size in breast infiltrating ductal carcinoma tissues (Yeh et al., 2006). On the other hand, p-STAT3 (ser) expression levels were more frequently seen in lower grade tumors in resected pancreatic ductal adenocarcinoma (Denley et al., 2013).

Several studies have shown the significance of ERK1/2 and suggested an oncogenic role in HNSCC (Wang et al., 2006; Lin et al., 2012; Gkouveris et al., 2014; Ji et al., 2014). Lin et al. (2012) and Ji et al. (2014) showed that ERK inhibition led to decreases in cell proliferation and increases in apoptosis in OSCC cells. Moreover, other authors suggested that overexpression of ERK1/2 may cause direct or indirect changes in cell proliferation in OSCC (Bancroft et al., 2001; Wang et al., 2006)

The results of the present study support the oncogenic role of phospho-ERK1/2 in HNSCC, in that high pERK1/2 immunoexpression levels correlate with poorly differentiated tumors in a statistically significant manner and could probably be considered as indicators of low differentiation. In agreement with our results, Mishima et al. (1998) performed an immunohistochemical study of 39 cases of OSCC and reported that overexpression of ERK1/2 correlates with the degree of tumor differentiation, reporting higher expression of ERK1/2 in poorly differentiated cases. Similar results were recorded by Wang et al. in 30 cases of tongue OSCC, adding that the increased expression levels of ERK1/2 were associated with elevated levels of cyclin D1 (Wang et al., 2006). In another immunohistochemical study of 101 HNSCC cases, Albanell et al. (2001) disclosed that higher expression levels of ERK1/2 were recorded in OSCC cases with distant lymph node metastasis and positively correlated with the expression of Ki-67, while Psyrri et al. (2014) found that activation of RAS/MAPK/ERK pathway was associated with resistance to chemotherapy with cetuximab in a tissue microarray HNSCC assay.

The role of JNK in oral cancer is still under investigation. A possible tumor suppressive role has been supported by Boivin et al. (2011), who showed that JNK mediates radiation-induced apoptosis in HNSCC stem and non-stem cells. Similarly, Li et al. (2013) demonstrated that JNK activation, induced by the drug AZD8055 in HNSCC, resulted in cell death, while its inhibition alleviated AZD8055-induced cytotoxic effects. Moreover, Yunoki et al. (2013) observed that silencing of BAG3 (chaperone protein of Hsp70) led to activation of JNK / Caspase-3 pathway, enhancing the sensitivity of OSCC cells in hyperthermia treatment therapy. In agreement with an oncosuppressive JNK role in OSCC, our previous study demonstrated that inhibition of JNK1/2 with either SP600125 treatment or specific siRNA silencing resulted in a dose-dependent rise in cell growth and viability in HNSCC cells, while opposite results were observed with JNK1/2 induction (Gkouveris et al., 2016).

In the present study, immunohistochemical staining for activated (phosphorylated) JNK was detected in 86% of cases with significant variations in the levels of expression. A significant difference in the intensity of staining was observed between moderately and poorly differentiated tumors, the latter showing weaker staining. Although other immunohistochemical parameters did not show significant differences, it could be speculated that loss of JNK activation may contribute to a less differentiated phenotype. A review of the literature did not reveal previous studies investigating the immunohistochemical expression of pJNK in HNSCC. As far as other tumor types are concerned, Kim et al. (2015) found increased expression of pJNK and p-cJun in hepatocarcinoma relative to normal liver tissues. On the other hand, Gulmann et al. (2009) reported that expression of phosphorylated JNK (as well as ERK and p-38) was decreased in colorectal cancer compared with normal tissue, but p-JNK downregulation reached significance only in the stromal compartment. Moreover, Yeh et al. (2006) demonstrated that decreased p-JNK1/2 expression in breast infiltrating ductal carcinoma (IDC) tissues was observed in 48.5% of cases, when compared to the nearby non-cancerous tissues, which correlated significantly with increased tumor grade and associated with a better overall survival of IDC.

Furthermore, we sought to examine the relationship between the immunohistochemical expression of pSTAT3, phosphorylated at either tyrosine or serine, and

MAPKs in OSCC. Statistically significant correlations between these molecules were mainly recorded in well differentiated tumors as well as in the whole cohort of tumors. In contrast, most of the correlations were lost in moderately and poorly differentiated tumors. In particular, positive statistical correlation was detected between pSTAT3(ser) and both pERK1/2 and pJNK. These findings were consistent with our previous studies, showing that both pERK1/2 and pJNK induce pStat3 serine phosphorylation in OSCC cells. Specifically, chemical or siRNA-induced inhibition of either ERK1/2 or JNK downregulated pSTAT3(ser), while induction of these molecules upregulated pSTAT3(ser) levels. In agreement, Guo et al. (2011) noticed a reduction in pSTAT3(ser) as a result of JNK inhibition in breast cancer cells.

Similarly, Tkach et al. (2013) showed that ERK1/2 inhibition suppresses pSTAT3(ser) in breast cancer cells, while Chen et al. (2008) demonstrated that induction of pSTAT3(ser) followed Erk1/2 activation in human bladder cancer cells.

Moreover, positive statistically significant correlation was found between pStat3(tyr) and pERK1/2 combined scores in all tumors, as well as in well differentiated cases. Nevertheless, in our previous *in vitro* study, it was shown that inhibition of Erk1/2 via U0126 or specific siRNA resulted in a moderate increase in pStat3(tyr), while Erk1/2 induction downregulated pStat3 tyrosine levels., in OSCC cells. However, it should be taken into consideration that the levels of immunohistochemical expression represent the net result of multiple, frequently interplaying parameters, involving the cancer cells as well as their environment; in contrast, pharmaceutical intervention in cell cultures is a more focused but rather simplified approach to investigate the interaction between biological molecules within cancer cells. Furthermore, both pSTAT3 tyrosine phosphorylation and ERK1/2 activation in OSCC could be regulated by common upstream molecules, such as EGFR (Molinolo et al., 2009; Sivanantham et al., 2016). Therefore, upstream signaling can drive a simultaneous upregula-tion of both pStat3(tyr) and pERK1/2, regardless of the possible negative crosstalk between the two molecules. Likewise, Zhen et al. (2014) suggested that inhibition of pEGFR expression resulted in reduced phosphorylation of downstream signaling molecules, including both ERK1/2 and STAT3, in OSCC cells. In addition, the observed positive statistically significant correlations between pJNK and pERK1/2 could be due to the fact that different MAPKs have several common upstream activators (such as cytokines and growth factors) (Maggioni et al., 2011). For example, Chang et al. (2012) described that epigallocatechin-3-gallate (EGCG) regulated phosphorylation of p38, JNK as well as ERK through pEGFR signaling in OSCC cells.

Positive statistical correlation was also detected between pSTAT3(ser) and p-STAT3(tyr), although limited to well differentiated tumors. The potent interaction between serine and tyrosine phosphorylation as well as the effect on STAT3 activation is still under investigation. While some studies have proposed a negative relationship between STAT3 serine and tyrosine phosphorylation (Venkatasubbarao et al., 2005; Wakahara et al., 2012), other investigators have suggested that STAT3 serine phosphorylation may contribute to STAT3 activity by increased nuclear translocation and maximized transcriptional activity (Aggarwal et al., 2009; Hazan-Halevy et al., 2010). In our previous study, simultaneous protein expression of both pSTAT3(ser) and p-STAT3(tyr) was detected by Western blot experiments in OSCC cell lines. Furthermore, Lin et al. (2014) demonstrated that increased expression of both pSTAT3(ser) and p-STAT3(tyr) is predictive of poorer clinical outcome in patients with glioblastoma tumors. Moreover, Denley et al. (2013) found that both high pSTAT3(ser) and p-STAT3(tyr) expression were associated with significantly decreased survival in pancreatic ductal adenocarcinoma, although only high pStat3 (Tyr) expression was an independent predictor of poor survival in multivariate analysis.

In summary, our data indicate that pERK1/2 and pSTAT3(tyr) overexpression could contribute to a less differentiated phenotype in OSCC. On the other hand, pJNK may support an opposite but less pronounced effect, while pSTAT3(ser) does not appear to correlate with the degree of differentiation. Positive correlations between MAPK and STAT3 levels may indicate a direct crosstalk which could regulate STAT3 activation through the effects of ERK1/2 and JNK activation and/or might imply that these molecules are downstream of shared activators. Understanding the role of STAT3 tyrosine or serine phosphorylation, as well as the complexity of ERK1/2 and JNK pathways and their crosstalk, may be key to determining their potential usefulness for diagnostic and/or therapeutic purposes.

References

Abroun S., Saki N., Ahmadvand M., Asghari F., Salari F. and Rahim F. (2015). STATs, an old story, yet mesmerizing. Cell J. 17, 395-411.

Aggarwal B.B., Kunnumakkara A.B., Harikumar K.B., Gupta S.R., Tharakan S.T., Koca C., Dey S. and Sung B. (2009). Signal transducer and activator of transcription-3, inflammation, and cancer, how intimate is the relationship? Ann. NY Acad. Sci. 1171, 59-76.

Aguzzi A., Maggioni D., Nicolini G., Tredici G., Gaini R.M. and Garavello W. (2009). MAP kinase modulation in squamous cell carcinoma of the oral cavity. Anticancer Res. 29, 303-308.

Albanell J., Codony-Servat J., Rojo F., Del Campo J.M., Sauleda S., Anido J., Raspall G., Giralt J., Rosello` J., Nicholson R.I., Mendelsohn J. and Baselga J. (2001). Activated extracellular signal-regulated kinases, association with epidermal growth factor receptor/ transforming growth factor alpha expression in head and neck squamous carcinoma and inhibition by anti-epidermal growth factor receptor treatments. Cancer Res. 61, 6500-6510.

Anjum R. and Blenis J. (2008). The RSK family of kinases, emerging roles in cellular signalling. Nat. Rev. Mol. Cell Biol. 9, 747-758.

Bancroft C.C., Chen Z., Dong G., Sunwoo J.B., Yeh N., Park C. and Van Waes C. (2001). Coexpression of proangiogenic factors IL-8

and VEGF by human head and neck squamous cell carcinoma involves coactivation by MEK-MAPK and IKK-NF-kappaB signal pathways. Clin. Cancer Res. 7, 435-442.

Bessard A., Frémin C., Ezan F., Fautrel A., Gailhouste L. and Baffet G. (2008). RNAi-mediated ERK2 knockdown inhibits growth of tumor cells *in vitro* and *in vivo*. Oncogene 27, 5315-5325.

Boivin A., Hanot M., Malesys C., Maalouf M., Rousson R., Rodriguez-Lafrasse C and Ardail D. (2011). Transient alteration of cellular redox buffering before irradiation triggers apoptosis in head and neck carcinoma stem and non-stem cells. PLoS One 6, e14558.

Chang L. and Karin M. (2001). Mammalian MAP kinase signalling cascades. Nature 410, 37-40.

Chang C.M., Chang P.Y., Tu M.G., Lu C.C., Kuo S.C., Amagaya S., Lee C.Y., Jao H.Y., Chen M.Y. and Yang J.S. (2012). Epigallocatechin gallate sensitizes CAL-27 human oral squamous cell carcinoma cells to the anti-metastatic effects of gefitinib (Iressa) via synergistic suppression of epidermal growth factor receptor and matrix metalloproteinase-2. Oncol. Rep. 28, 1799-1807.

Chen F. (2012). JNK-induced apoptosis, compensatory growth, and cancer stem cells. Cancer Res. 72, 379-386.

Chen Z., Gibson T.B., Robinson F., Silvestro L., Pearson G., Xu B., Wright A., Vanderbilt C. and Cobb M.H. (2001). MAP kinases. Chem. Rev. 101, 2449-2476.

Chen R.J., Ho Y.S., Guo H.R. and Wang Y.J. (2008). Rapid activation of Stat3 and ERK1/2 by nicotine modulates cell proliferation in human bladder cancer cells. Toxicol. Sci. 104, 283-293.

Chen F., Beezhold K. and Castranova V. (2009). JNK1., a potential therapeutic target for hepatocellular carcinoma. Biochim Biophys Acta 1796, 242-251.

Chen B., Liu J., Chang Q., Beezhold K., Lu Y. and Chen F. (2013). JNK and STAT3 signaling pathways converge on Akt-mediated phosphorylation of EZH2 in bronchial epithelial cells induced by arsenic. Cell Cycle 12, 112-121.

Chung J., Uchida E., Grammer T.C. and Blenis J. (1997). STAT3 serine phosphorylation by ERK-dependent and -independent pathways negatively modulates its tyrosine phosphorylation. Mol. Cell. Biol. 17, 6508-6516.

Denley S.M., Jamieson N.B., McCall P., Oien K.A., Morton J.P., Carter C.R., Edwards J. and McKay C.J. (2013). Activation of the IL-6R/Jak/stat pathway is associated with a poor outcome in resected pancreatic ductal adenocarcinoma. J. Gastrointest. Surg. 17, 887-898.

Dhillon A.S., Hagan S., Rath O. and Kolch W. (2007). MAP kinase signalling pathways in cancer. Oncogene 26, 3279-3290.

Gkouveris I., Nikitakis N., Karanikou M., Rassidakis G. and Sklavounou A. (2014). Erk1/2 activation and modulation of STAT3 signaling in oral cancer. Oncol. Rep. 32, 2175-2182.

Gkouveris I., Nikitakis N. and Sauk J. (2015). STAT3 signaling in cancer. J. Cancer Ther. 6, 709-726.

Gkouveris I., Nikitakis N., Karanikou M., Rassidakis G. and Sklavounou A. (2016). JNK1/2 expression and modulation of STAT3 signaling in oral cancer. Oncol. Lett. 12, 699-706.

Gross N.D., Boyle J.O., Du B., Kekatpure V.D., Lantowski A., Thaler H.T., Weksler B.B., Subbaramaiah K. and Dannenberg A.J. (2007). Inhibition of Jun NH2-terminal kinases suppresses the growth of experimental head and neck squamous cell carcinoma. Clin. Cancer Res. 13, 5910-5917.

Gu F., Ma Y., Zhang Z., Zhao J., Kobayashi H., Zhang L. and Fu L. (2010). Expression of Stat3 and Notch1 is associated with cisplatin resistance in head and neck squamous cell carcinoma. Oncol. Rep. 23, 671-676.

Gulmann C., Sheehan K.M., Conroy R.M., Wulfkuhle J.D., Espina V., Mullarkey M.J., Kay E.W., Liotta L.A. and Petricoin E.F. 3rd. (2009). Quantitative cell signalling analysis reveals down-regulation of MAPK pathway activation in colorectal cancer. J. Pathol. 218, 514-5149.

Guo W., Wu S., Wang L., Wei X., Liu X., Wang J., Lu Z., Hollingshead M. and Fang B. (2011). Antitumor activity of a novel oncrasin analogue is mediated by JNK activation and STAT3 inhibition. PLoS One 6,e28487.

Hazan-Halevy I., Harris D., Liu Z., Liu J., Li P., Chen X., Shanker S., Ferrajoli A., Keating MJ. and Estrov Z. (2010). STAT3 is constitutively phosphorylated on serine 727 residues., binds DNA., and activates transcription in CLL cells. Blood 115, 2852-2863.

Jewett A., Head C. and Cacalano N.A. (2006). Emerging mechanisms of immunosuppression in oral cancers. J. Dent. Res. 85, 1061-1073.

Ji WT., Chen HR., Lin CH., Lee JW. and Lee CC. (2014). Monocyte chemotactic protein 1 (MCP-1) modulates pro-survival signaling to promote progression of head and neck squamous cell carcinoma. PLoS One 9, e88952.

Kijima T., Niwa H., Steinman R.A., Drenning S.D., Gooding W.E., Wentzel A.L., Xi S. and Grandis J.R. (2002). STAT3 activation abrogates growth factor dependence and contributes to head and neck squamous cell carcinoma tumor growth *in vivo*. Cell Growth Differ. 13, 355-362.

Kim J.B., Park S.Y., Kim H.R., Ahn Y.H., Jee H.G., Lee J.H., Yu S.J., Lee H.S., Lee M., Yoon J.H. and Kim Y.J. (2015). JNK signaling in epatocarcinoma cells is associated with the side population upon treatment with anticancer drugs. Mol. Med. Rep. 11, 263-268.

Kim TW., Michniewicz M., Bergmann DC. and Wang ZY. (2012). Brassinosteroid regulates stomatal development by GSK3-mediated inhibition of a MAPK pathway. Nature 482, 419-22.

Lai S.Y. and Johnson F.M. (2010). Defining the role of the JAK-STAT pathway in head and neck and thoracic malignancies, implications for future therapeutic approaches. Drug Resist. Updat. 13, 67-78.

Lee T.L., Yeh J., Van Waes C. and Chen Z. (2006). Epigenetic modification of SOCS-1 differentially regulates STAT3 activation in response to interleukin-6 receptor and epidermal growth factor receptor signaling through JAK and/or MEK in head and neck squamous cell carcinomas. Mol. Cancer Ther. 5, 8-19.

Leeman R.J., Lui V.W. and Grandis J.R. (2006). STAT3 as a therapeutic target in head and neck cancer. Expert Opin. Biol. Ther. 6, 231-241.

Li Q., Song X.M., Ji Y.Y., Jiang H. and Xu L.G. (2013). The dual mTORC1 and mTORC2 inhibitor AZD8055 inhibits head and neck squamous cell carcinoma cell growth *in vivo* and *in vitro*. Biochem. Biophys. Res. Commun. 440, 701-706.

Lim C.P. and Cao X. (1999). Serine phosphorylation and negative regulation of Stat3 by JNK. J. Biol. Chem. 274, 31055-31061.

Lin Y.C., Wu M.H., Wei T.T., Chuang S.H., Chen K.F., Cheng A.L. and Chen C.C. (2012). Degradation of epidermal growth factor receptor mediates dasatinib-induced apoptosis in head and neck squamous cell carcinoma cells. Neoplasia 14, 463-475.

Lin G.S., Chen Y.P., Lin Z.X., Wang X.F., Zheng Z.Q. and Chen L. (2014). STAT3 serine 727 phosphorylation influences clinical outcome in glioblastoma. Int. J. Clin. Exp. Pathol. 7, 3141-3149.

Macha M.A., Matta A., Kaur J., Chauhan S.S., Thakar A., Shukla N.K., Gupta S.D. and Ralhan R. (2011). Prognostic significance of nuclear pSTAT3 in oral cancer. Head Neck 33, 482-489.

Maggioni D., Gaini R., Nicolini G., Tredici G. and Garavello W. (2011). MAPKs activation in head and neck squamous cell carcinomas. Oncol. Rev. 5, 223-231.

Mali S.B. (2015). Review of STAT3 (Signal Transducers and Activators of Transcription) in head and neck cancer. Oral Oncol. 51, 565-569.

Masuda M., Suzui M., Yasumatu R., Nakashima T., Kuratomi Y., Azuma K., Tomita K., Komiyama S. and Weinstein I.B. (2002). Constitutive activation of signal transducers and activators of transcription 3 correlates with cyclin D1 overexpression and may provide a novel prognostic marker in head and neck squamous cell carcinoma. Cancer Res. 62, 3351-3355.

Mendoza M.C., Er E.E. and Blenis J. (2011). The Ras-ERK and PI3K-mTOR pathways, cross-talk and compensation. Trends Biochem. Sci. 36, 320-328.

Mishima K., Yamada E., Masui K., Shimokawara T., Takayama K., Sugimura M. and Ichijima K. (1998). Overexpression of the ERK/MAP kinases in oral squamous cell carcinoma. Mod. Pathol. 11, 886-891.

Molinolo A.A., Amornphimoltham P., Squarize C.H., Castilho R.M., Patel V. and Gutkind J.S. (2009). Dysregulated molecular networks in head and neck carcinogenesis. Oral Oncol. 45, 324-334.

Naher L., Kiyoshima T., Kobayashi I., Wada H., Nagata K., Fujiwara H., Ookuma Y.F., Ozeki S., Nakamura S. and Sakai H. (2012). STAT3 signal transduction through interleukin-22 in oral squamous cell carcinoma. Int. J. Oncol. 41, 1577-1586

Nikitakis N.G., Siavash H. and Sauk J.J. (2004). Targeting the STAT pathway in head and neck cancer, recent advances and future prospects. Curr. Cancer Drug Targets 4, 637-651.

Obajimi O. and Melera P. (2010). Suppression of ERK1/2 with siRNA restores drug sensitivity in DU145 cells selected for resistance to AG2034. Cancer Res. 70 (Suppl 1), Abstract 77.

Psyrri A., Lee J.W., Pectasides E., Vassilakopoulou M., Kosmidis E.K., Burtness B.A., Rimm D.L., Wanebo H.J. and Forastiere A.A. (2014). Prognostic biomarkers in phase II trial of cetuximab-containing induction and chemoradiation in resectable HNSCC, Eastern cooperative oncology group E2303. Clin. Cancer Res. 20, 3023-3032.

Reich NC. and Liu L. (2006). Tracking STAT nuclear traffic. Nat. Rev. Immunol. 6, 602-612.

Sau A., Filomeni G., Pezzola S., D'Aguanno S., Tregno F.P., Urbani A., Serra M., Pasello M., Picci P., Federici G. and Caccuri A.M. (2012). Targeting GSTP1-1 induces JNK activation and leads to apoptosis in cisplatin-sensitive and -resistant human osteosarcoma cell lines. Mol. Biosyst. 8, 994-1006.

Sen M., Joyce S., Panahandeh M., Li C., Thomas S.M., Maxwell J., Wang L., Gooding W.E., Johnson D.E. and Grandis J.R. (2012). Targeting Stat3 abrogates EGFR inhibitor resistance in cancer. Clin. Cancer Res. 18, 4986-4996.

Shah N.G., Trivedi T.I., Tankshali R.A., Goswami J.A., Jetly D.H., Kobawala T.P., Shukla S.N., Shah P.M. and Verma R.J. (2006). Stat3 expression in oral squamous cell carcinoma,association with clinicopathological parameters and survival. Int. J. Biol. Markers 21, 175-183.

Shah N.G., Trivedi T.I., Tankshali R.A., Goswami J.V., Jetly D.H., Shukla S.N., Shah P.M. and Verma R.J. (2009). Prognostic significance of molecular markers in oral squamous cell carcinoma, a multivariate analysis. Head Neck 31, 1544-1556.

Siavash H., Nikitakis N.G. and Sauk J.J. (2004). Abrogation of IL-6-mediated JAK signalling by the cyclopentenone prostaglandin 15d-PGJ(2) in oral squamous carcinoma cells. Br. J. Cancer 91, 1074-1080.

Sivanantham B., Sethuraman S. and Krishnan U.M. (2016). Combinatorial effects of curcumin with an anti-neoplastic agent on head and neck squamous cell carcinoma through the regulation of EGFR-ERK1/2 and apoptotic signaling pathways. ACS Comb. Sci. 18, 22-35.

Smalley K.S. (2003). A pivotal role for ERK in the oncogenic behavior of malignant melanoma? Int. J. Cancer 104, 527-532.

Sui X., Kong N., Ye L., Han W., Zhou J., Zhang Q., He C. and Pan H. (2014). p38 and JNK MAPK pathways control the balance of apoptosis and autophagy in response to chemotherapeutic agents. Cancer Lett. 344,174-179.

Tkach M., Rosemblit C., Rivas M.A., Proietti C.J., Díaz Flaqué M.C., Mercogliano M.F., Beguelin W., Maronna E., Guzmán P., Gercovich F.G., Deza E.G., Elizalde P.V. and Schillaci R. (2013). p42/p44 MAPK-mediated Stat3Ser727 phosphorylation is required for progestin-induced full activation of Stat3 and breast cancer growth. Endocr. Relat. Cancer 20, 197-212.

Trivedi T.I., Tankshali R.A., Goswami J.V., Shukla S.N., Shah P.M. and Shah N.G. (2011). Identification of site-specific prognostic biomarkers in patients with oral squamous cell carcinoma. Neoplasma 58, 217-226.

Venkatasubbarao K., Choudary A. and Freeman J.W. (2005). Farnesyl transferase inhibitor (R115777)-induced inhibition of STAT3(Tyr705) phosphorylation in human pancreatic cancer cell lines require extracellular signal-regulated kinases. Cancer Res. 65, 2861-2871.

Wakahara R., Kunimoto H., Tanino K., Kojima H., Inoue A., Shintaku H. and Nakajima K. (2012). Phospho-Ser727 of STAT3 regulates STAT3 activity by enhancing dephosphorylation of phospho-Tyr705 largely through TC45. Genes Cells 17, 132-145.

Wang L., Liu T., Nishioka M., Aguirre R.L., Win S.S. and Okada N. (2006). Activation of ERK1/2 and cyclin D1 expression in oral tongue squamous cell carcinomas, relationship between clinicopathological appearances and cell proliferation. Oral Oncol. 42, 625-631.

Xiong A., Yang Z., Shen Y., Zhou J. and Shen Q. (2014). Transcription factor STAT3 as a novel molecular target for cancer prevention. Cancers (Basel) 6, 926-957.

Yeh Y.T., Hou M.F., Chung Y.F., Chen Y.J., Yang S.F., Chen D.C., Su J.H. and Yuan S.S. (2006). Decreased expression of phosphorylated JNK in breast infiltrating ductal carcinoma is associated with a better overall survival. Int. J. Cancer 118, 2678-2684.

Yeh Y.T., Ou-Yang F., Chen I.F., Yang S.F., Wang Y.Y., Chuang H.Y., Su J.H., Hou M.F. and Yuan S.S. (2006). STAT3 ser727 phosphorylation and its association with negative estrogen receptor status in breast infiltrating ductal carcinoma. Int. J. Cancer 118, 2943-2947.

Yunoki T., Kariya A., Kondo T., Hayashi A. and Tabuchi Y. (2013). The combination of silencing BAG3 and inhibition of the JNK pathway enhances hyperthermia sensitivity in human oral squamous cell carcinoma cells. Cancer Lett. 335, 52-57.

Zhang Q., Raje V., Yakovlev V.A., Yacoub A., Szczepanek K., Meier J., Derecka M., Chen Q., Hu Y., Sisler J., Hamed H., Lesnefsky E.J., Valerie K., Dent P. and Larner A.C. (2013). Mitochondrial localized Stat3 promotes breast cancer growth via phosphorylation of serine 727. J. Biol. Chem. 288, 31280-31288.

Zhen L., Fan D., Yi X., Cao X., Chen D. and Wang L. (2014). Curcumin inhibits oral squamous cell carcinoma proliferation and invasion via EGFR signaling pathways. Int. J. Clin. Exp. Pathol. 7, 6438-6446.

Accepted January 16, 2017